JOURNAL OF GEOPHYSICAL RESEARCH, VOL. 101, NO. D11, PAGES 16,731–16,736, JULY 20, 1996

Colors of contrails from fuels with different sulfur contents

K. Gierens and U. Schumann

Deutsche Forschungsanstalt für Luft- und Raumfahrt, Institut für Physik der Atmosphäre, Oberpfaffenhofen, Germany

Abstract. During a recent flight experiment, contrails were produced from fuels with normal and very high sulfur content. A color effect was observed [*Schumann et al.*, 1996]. When observed with the Sun in the back, the low-sulfur contrail appeared grey with weak contrast against the cloud deck underneath, whereas the high-sulfur contrail appeared slightly brown with higher contrast. In order to give an explanation, we compute the optical properties of the soot-containing droplets in the contrails and perform a simple radiative transfer computation. We find that the degree of activation of the soot particles is the basic parameter for the explanation of color and contrast of the contrails. It determines the size and number concentration of the droplets, which both in turn determine the optical properties of the contrail as a whole. For the visual appearance of the relatively optically thin contrails ($\tau \lesssim 1.2$) the soot volume fraction in the droplets plays only a minor role.

1. Introduction

Contrails are visible clouds which form in the exhaust plumes of aircraft engines. Because of the large and increasing number of aircraft causing contrails which occasionally obscure a large fraction of the sky at least regionally, contrails may have a climatological impact [*Schumann*, 1994]. The exhaust also causes an invisible aerosol trail [*Hofmann and Rosen*, 1978] which contributes condensation nuclei and possibly affects air chemistry [*World Meteorological Organization*, 1995]. The properties and impact of contrails and aerosols depend on the nature and number of particles in the exhaust plume and on the ambient air conditions. Contrails are expected to form when isobaric mixing between the hot and humid exhaust plume and the cold ambient air leads to a mixture reaching saturation with respect to liquid water so that cloud droplets form which then might freeze [see, for example, *Appleman*, 1953]. The cloud condensation nuclei required for this process may depend on the sulfur content of the fuel burnt in the engines. Jet fuels contain sulfur at a mass fraction between about 2 and 1000 ppm [*Busen and Schumann*, 1995], with a specification limit of 3000 ppm, and average values near 420 ppm [*Schumann*, 1994]. Hence, engines emit sulfurous gases, which get partly converted to sulfuric acid and may contribute to particle formation [*Reiner and Arnold*, 1993], but the details of this process are unknown.

In the exhaust plume, sulfuric acid is highly supersaturated at the temperatures of common flight levels [*Miake-Lye et al.*, 1994]. Thus it can undergo binary homogeneous nucleation (H_2SO_4/H_2O) which may yield a large number of small sulfuric acid solution droplets (a few 10^{10} cm^{-3}) or lead to subsequent heterogeneous condensation on soot particles or ions in the exhaust. *Kärcher et al.* [1995] have shown that a contrail does not become visible at threshold conditions when homogeneous H_2SO_4/H_2O nucleation is the only ice-forming process. This indicates that activated soot particles might play an essential role in the formation of visible contrails. In fact, *Hagen et al.* [1992] measured a concentration of $10^5 - 10^6$ soot particles cm^{-3} of 30-100 nm size directly behind the engine exit. Although pure carbon is hydrophobic, soot can become activated by a variety of exhaust gases including the sulfuric gases SO_2 and H_2SO_4 [*Kärcher et al.*, 1996; see also *Parungo et al.*, 1992; *Wyslouzil et al.*, 1994; *DeMott*, 1990; *Zhao and Turco*, 1995].

In order to identify the impact of fuel sulfur content on contrail formation, two experiments were performed recently. In both experiments the contrails were observed as forming behind the twin-engine jet aircraft ATTAS [*Busen and Schumann*, 1995]. Each engine burnt fuels from separate tanks of the ATTAS with different sulfur contents. In the first experiment, *Busen and Schumann* [1995] observed the contrails visually for fuels with 2 and 250 ppm sulfur content and found no visible difference. In the second experiment, *Schumann et al.* [1996] measured the concentration of small particles in the plumes and found measurable and visible differences when burning fuels with 170 and 5500 ppm sulfur content. The higher sulfur emission caused a larger optical thickness of the contrail shortly after onset, with a slightly brown colored contrail when observed from above with the Sun in the back and a bright deck of low clouds below the contrails, and more contrast when viewed from below against the Sun. They also measured the plume width (about 2 m) and determined the maximum amount of liquid water per air mass available for condensation (0.143 $g\,kg^{-1}$) in the young contrails, and estimated the median diameter and the number density of soot particles (about 60 nm and 7×10^{11} m^{-3}). In order to learn about the particle formation process, the present paper aims in explaining the observed differences in the optical properties of the contrails for different fuel sulfur contents.

Paper number 96JD01169.
0148-0227/96/96JD-01169$09.00

To explain the observed differences between the high- and low-sulfur contrails in the second ATTAS experiment, *Schumann et al.* [1996] proposed the following scenario: both engines exhaust a large amount of soot particles together with sulfur oxides and water vapor. Normally, the soot is hydrophobic, but under the influence of the sulfur (details are unknown) more or less of it gets hydrophylic. It is assumed that in the high-sulfur contrail almost all soot particles become water attracting and that they determine the number of droplets formed, hence $N_{drop} \approx N_{soot}$. For the low-sulfur contrail it is assumed that only a fraction $a \approx 0.1$ of the soot particles gets hydrophilic, yielding $N_{drop} = aN_{soot}$. When all the water vapor that was actually available for condensation in the plume condensed out on the activated soot particles, the droplets in the high-sulfur contrail have a mean diameter of $d_H = 0.56\ \mu$m; in the low-sulfur contrail they are larger, $d_L = 1.21\ \mu$m for $a = 0.1$. The volume fraction of soot in the droplets is $v_H = 10^{-3}$ and $v_L = 10^{-4}$ for the high (index H) and low-sulfur (index L) contrail, respectively.

On the basis of previous investigations, it can be expected that different sizes [e.g. *Husar and White,* 1976] and soot contents [e.g., *Chýlek et al.,* 1984] of the droplets can lead to the different visible appearances of the two contrails that were observed in the experiment and documented on photographs and video films. The contrail colors are quantified in the next section. In sections 3 and 4 we first derive the optical properties of soot contaminated droplets, and then we compute from these some radiative transfer properties of the contrails. Discussion and conclusions follow in sections 5 and 6.

2. Quantitative Determination of Contrail Colors

Since no color meter was available in the ATTAS experiment, the contrail colors have been determined visually by matching the colors on the photographs as reproduced by *Schumann et al.* [1996] with printed standard colors from DIN 6164. In this color system, colors are distinguished by three properties, hue T, saturation S, and degree of darkness D. The colors are designated $T : S : D$. In a chromaticity diagram as shown in Figure 1 [see, for example, *Richter,* 1976; *Judd and Wyszecki,* 1975; *Middleton,* 1952], lines of constant hue T are straight lines, all beginning from a common center (C in Figure 1), which is the locus of the hueless color (e.g., white). The lines of constant saturation S are deformed circles around this center. Therefore, pairs $T : S$ can easily be converted into coordinates (x, y) on the chromaticity diagram. The DIN 6164 color system (version 1962) is valid for the CIE (Commission Internationale de l'Éclairage) standard daylight C, that is, the coordinates of C define the origin of the T lines in the chromaticity diagram. It is, therefore, convenient to use a transformed chromaticity diagram (x_C, y_C) in which the hueless source C has the coordinates $(\frac{1}{3}, \frac{1}{3})$. The transformation is described in *Richter* [1976, Anhang 1]. In the present paper we use the transformed CIE 1931 chromaticity diagram.

The matching of the contrail colors from the photos with the standard colors bore some problems, which lead to a kind of error box around the determined chromaticity coordinates.

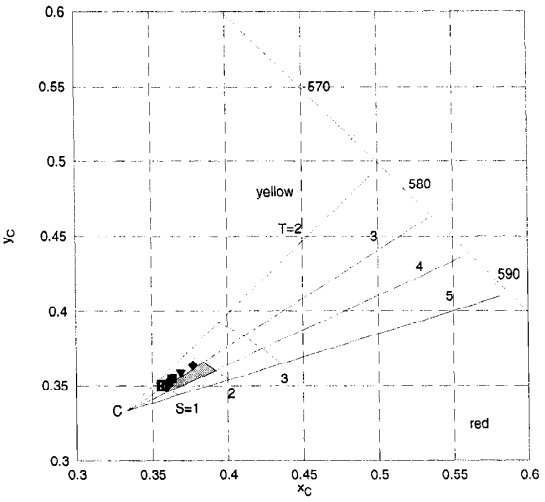

Figure 1. Yellow-orange-red section of the color chart with standard source C at the center ($x_C = y_C = \frac{1}{3}$). The four rays labelled T=2, 3, 4, 5 are the corresponding hues of the DIN 6164 color system, the arcs labelled S=1, 2, 3 are the saturation values. The degree of darkness is not given in the color chart. The line with ticks is the spectrum locus, that is, the locus of pure (monochromatic) colors; some wavelengths in nanometer are indicated. The standard colors that most closely matched the contrail colors on the photographs, $T : S = 3 - 4 : 1$ and $3 - 4 : 2$ for the low- and high-sulfur contrails, respectively, are located at the four corners of the grey-shadowed area. The symbols refer to the computed colors: open symbols, low-sulfur; solid symbols, high-sulfur; squares, δ droplet size distribution, viewing angle 0°; diamonds, δ, 70°; circle, Γ, 0°; triangle, Γ, 70°. The results for the L contrail with Γ distribution are not shown since they are nearly coincident with those of the δ distribution.

(1) The photographs are glossy, the printed standard colors are not. (2) The contrails are translucent and have structure, whereas the standards are opaque and structureless. (3) The DIN uses standard source C as the hueless reference color, which is a mean daylight spectrum at ground. However, for contrails we expect an illumination with a higher contribution of blue light. Unfortunately, these problems cannot be quantified, thus we decided not to draw error boxes around the determined chromaticity coordinates.

For the two contrails (L and H) we found the color match to be closest with $T : S : D = 3 - 4 : 1 : 4$ for contrail L and $3 - 4 : 2 : 5$ for contrail H. $T = 3 - 4$ is in the orange part of the chromaticity diagram, $S = 1$ and $S = 2$ are relatively low saturations (a maximum of 7 is possible for $T = 3$ and 4), in other words, the contrail colors are rather impure. $D = 4$ and 5 mean a medium darkness ($D = 0$ is white and $D = 10$ is black). The positions of the determined colors are the four corners of the grey-shadowed area in the chromaticity diagram (Figure 1). The task is now to see whether the computed contrail colors that result from the above mentioned scenario fall near to these points or not.

3. Radiative Properties of Soot-Containing Droplets

Using the Mie theory, we have computed the optical properties of soot-containing drops for the visible part of the spectrum, 400 nm$\leq \lambda \leq$750 nm. We have applied the technique described by *Chýlek et al.* [1984] for the computation of the complex index of refraction of the water/soot mixture, using the refraction indices for pure water from the tabulation of *Hale and Querry* [1973] and a grey (wavelength independent) refraction index for soot taken as $m_C = 1.57 - 0.47i$ [*Haynes and Wagner,* 1981]. We do not expect a shell configuration (water inside, soot outside, see for example, *Chýlek and Hallett,* [1992]) for a contrail, since this configuration typically results when slowly falling (preexisting) drops capture soot particles. In a contrail, instead, the soot particles, acting as nucleation sites, must be expected to be immersed within the droplets. Having mean diameter of 60 nm in the dry plume, the soot particles may get segregated when they are dissolved in water [*Parungo et al.,* 1992]. Thus, we assume that the graphite particles in the droplets obey a Γ-size distribution with mode diameter $d_m = 20$ nm and width parameter $\alpha = 3$. The calculated refraction indices m are compiled in Table 1. From these we have computed (again using Mie theory) the extinction efficiency $Q_{ext}(\lambda)$, single scattering albedo $\varpi(\lambda)$, and asymmetry factor $g(\lambda)$. We have considered two droplet size distributions: (1) a δ-type distribution (i.e., all droplets have equal size d_H and d_L, respectively), and (2) a moderately broad ($\alpha = 3$) Γ-size distribution (both distributions giving the same concentration of liquid water). Iridescence observations of *Sassen* [1979] indicate a narrow droplet size distribution. The resulting single scattering albedo for the δ-type distribution are listed also in Table 1. (For pure water droplets $\varpi(\lambda) = 1$ in the visible part of the spectrum.) Extinction efficiencies Q_{ext} and asymmetry factors g are plotted in Figures 2 and 3 versus wavelength. It is seen that these properties display contrary wavelength dependence in the visible part of the spectrum, in particular when the size distribution is narrow. It can, therefore, be expected that contrails composed of such particles differ in their visual appearance. It must be noted, however, that the differences in the $Q_{ext}(\lambda)$ and $g(\lambda)$ curves arise mainly from the different size of the droplets in the two contrails, not from the soot content. The corresponding values of Q_{ext} and g for pure water droplets differ from those in Figures 2 and 3 by less than 0.2%.

Table 1. Optical Properties of Droplets in the High- and Low-Sulfur Contrail

λ[nm]	$\Re(m)$	$\Im(m)$	ϖ_0
	Low-Sulfur Contrail		
400	1.339	$-4.526\cdot10^{-5}$	0.999121
450	1.337	$-4.505\cdot10^{-5}$	0.999430
500	1.335	$-4.486\cdot10^{-5}$	0.999572
550	1.333	$-4.468\cdot10^{-5}$	0.999644
600	1.332	$-4.454\cdot10^{-5}$	0.999680
650	1.331	$-4.442\cdot10^{-5}$	0.999712
700	1.331	$-4.434\cdot10^{-5}$	0.999721
750	1.330	$-4.436\cdot10^{-5}$	0.999737
	High-Sulfur Contrail		
400	1.339	$-4.524\cdot10^{-4}$	0.997372
450	1.337	$-4.503\cdot10^{-4}$	0.997336
500	1.335	$-4.483\cdot10^{-4}$	0.997241
550	1.333	$-4.465\cdot10^{-4}$	0.997099
600	1.332	$-4.451\cdot10^{-4}$	0.996864
650	1.331	$-4.438\cdot10^{-4}$	0.996699
700	1.331	$-4.429\cdot10^{-4}$	0.996562
750	1.330	$-4.420\cdot10^{-4}$	0.996318

Real and imaginary part of refraction index m, and single scattering albedo ϖ_0.

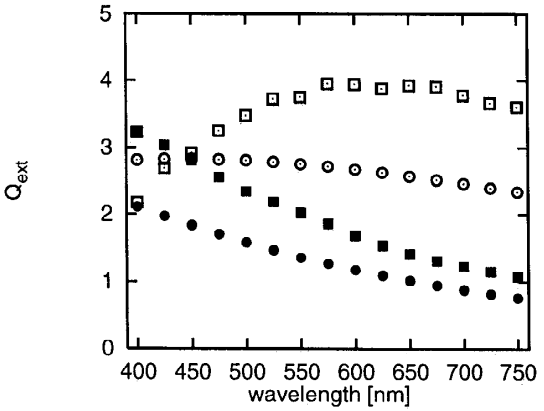

Figure 2. Extinction efficiency of droplets in the high (solid symbols) and low-sulfur (open symbols) contrails versus wavelength for two droplet size distributions: δ-type with $d_H = 0.56$ μm and $d_L = 1.21$ μm (squares) and Γ-distribution (circles).

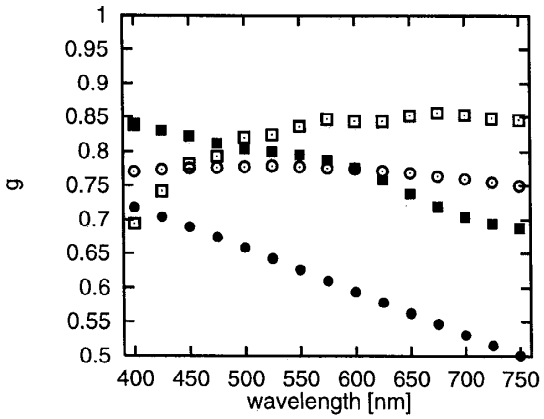

Figure 3. Asymmetry factor for droplets in the high (solid symbols) and low-sulfur (open symbols) contrails versus wavelength. Squares refer to a δ-type size distribution, circles to a Γ-distribution as in Figure 1.

4. Radiative Transfer Properties of the two Contrails

We postulate a transmission situation: the bright cloud deck underneath the contrail is the light source, the contrail is the color filter, and the observer flying above the contrail is the detector. In the previous section we computed the optical properties of the single droplets that the contrails consist of. Now we compute the optical depth of the contrails as a whole:

$$\tau_X(\lambda) = D \sec\zeta \, N_{drop,X} \times \times \int_0^\infty (\pi/4) d^2 Q_{ext}(\lambda, d) \, n_X(d) \, \mathrm{d}d, \quad (1)$$

where the index X stands for either L or H, D is the diameter of the contrail (here $D = 2$ m), $N_{drop,L} = 7 \times 10^{10}$ m^{-3}, $N_{drop,H} = 7 \times 10^{11}$ m^{-3}, and $n_X(d)$ is the normalized droplet size distribution (δ- or Γ-type). The factor $\sec\zeta = (\cos\zeta)^{-1}$ accounts for the oblique viewing direction, $90° - \zeta$ being the angle between the line of sight and the contrail axis. The contribution of the interstitial soot in the L contrail has been neglected because its optical depth is of the order 10^{-3}.

If the contrail was a clear medium (i.e., no scattering) then the transmission $e^{-\tau}$ was the relevant quantity for the determination of the color. However, since the contrail is a turbid (i.e., scattering) medium, it is necessary to take the scattering into account. Indeed, scattering here is much more important than true absorption since the optical depth is low (generally < 1.2) and the single scattering albedo is near unity. Thus, we should now set up a radiative transfer model for the observed situation and compute the colors. However, this method is not viable since we do not have enough information about the situation. In particular, neither do we know the spatial structure of the contrails nor the light field that illuminates them. Therefore, we resort to a much simpler approach that yet takes account of the scattering properties of the droplets. The light emerging from the bright cloud deck underneath and transmitted through the contrail consists of two parts: (1) the photons that cross the contrail without any interaction with the droplets or ice crystals (probability $e^{-\tau}$) and (2) the photons that are scattered once into the forward direction with probability $(1 - e^{-\tau}) \times f$, where f is the fraction of photons scattered into the forward direction per interaction event. (Multiple scattering is ignored because of the relatively low optical thickness of the contrails.) *Joseph et al.* [1976] gave for f the expression $f = g^2 \varpi_0$, which is used here. The probability for a photon to cross the contrail either without any interaction or by forward scattering is therefore $e^{-\tau'}$ with the scaled optical depth

$$\tau' = \tau \times (1 - g^2 \varpi_0). \quad (2)$$

For a size distribution this reads:

$$\tau'_X(\lambda) = D \sec\zeta \, N_{drop,X} \int_0^\infty (\pi/4) d^2 Q_{ext}(\lambda, d) \times \times [1 - g^2(\lambda, d) \varpi_0(\lambda, d)] \, n_X(d) \, \mathrm{d}d. \quad (3)$$

The scaled optical depths (for $\zeta = 0°$) are plotted versus wavelength in Figure 4. It is seen, that τ' increases with decreasing wavelength for the high-sulfur contrail, whereas it remains nearly constant over the whole visual spectrum in the low-sulfur contrail. This result holds for both droplet size distributions that we have considered. Thus, blue light is subject to stronger extinction than red light in the H contrail which explains a brownish hue. On the other hand, the flat spectrum in the L contrail explains why the color of this contrail is nearly grey. Furthermore, we see that generally the H contrail possesses higher optical depth than the L contrail (both τ and τ'). This fact explains the darker appearance of the H contrail against the bright cloud deck underneath. The corresponding colors, that is, the coordinates in the CIE 1931 chromaticity diagram have been calculated from the scaled optical depths with

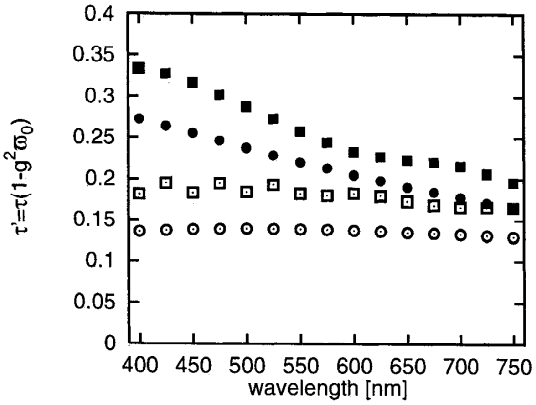

Figure 4. Scaled optical depth along the diameter of the high (solid symbols) and low-sulfur (open symbols) contrails versus wavelength for δ-type (squares) and Γ-size distribution (circles).

$$X = \int_{400\ \mathrm{nm}}^{750\ \mathrm{nm}} \exp[-\tau'(\lambda)] \, \overline{x}(\lambda) \, \mathrm{d}\lambda, \quad (4)$$

and similar expressions for Y and Z, where $\overline{x}(\lambda)$, $\overline{y}(\lambda)$, and $\overline{z}(\lambda)$ are the CIE 1931 tristimulus values [*Richter,* 1976; *Judd and Wyszecki,* 1975; *Middleton,* 1952]. The chromaticity coordinates follow from

$$x = X/(X + Y + Z), \quad (5)$$

again with similar expressions for y and $z = 1 - x - y$. The triple (x, y, z) has then been converted into (x_C, y_C, z_C) following the procedure described by *Richter* [1976, Anhang 1] and the resulting values were marked in the chromaticity diagram of Figure 1.

Let us first look at the results for the low-sulfur contrail (open symbols). For both the δ- and Γ-type (not shown) distributions and for viewing angles of 0° (square) and 70° (diamond), the determined chromaticity coordinates fall in the immediate vicinity of the point $T : S = 3 : 1$, which is one of the DIN 6164 standard colors that most closely matched the color of the L contrail on the photographs. For this contrail we can state that observation and computation are in excellent agreement. For the high-sulfur contrail we

find computed color coordinates (solid symbols) along the $T = 3$ ray between $S = 1$ and $S = 2$. We find that the color is the more saturated (1) the narrower the droplet size distribution is (δ: square and diamond, Γ: circle and triangle) and (2) the larger the viewing angle is (0°: square and circle, 70°: diamond and triangle). The second of these results is confirmed by the observations. The H contrail had a less saturated color when viewed directly from above. The computed color coordinates for the H contrail do not reach the $S = 2$ line in the diagram, which yielded the best color match between the photos and the standard colors. However, printed standard colors for saturation values intermediate between $S = 1$ and 2 do not exist, but we think that we also found for the H contrail good agreement between observation and computed result.

5. Discussion

We have conducted three further test calculations. First, in order to check the influence of the soot in the droplets, we have computed the chromaticity coordinates of a hypothetical contrail that consists of pure water droplets with the same size and number density than the H contrail. The results were almost identical (differences less than 1%). This shows that it is not the soot volume fraction within the drops nor the distribution of the soot inside them (segregation or not) what determines the contrail color. Instead, it is the droplet size distribution and number density that determines the color. These in turn are controlled by the degree of activation of the soot particles that leave the engines, and by the amount of condensable water in the expanding plume. This means also, that the exact value of the soot refraction index does not matter for the contrail color (there is a considerable spread in the value of m_C in the literature, see Table 1 of *Janzen* [1979]). Values of Q_{ext}, ϖ_0, and g differ by less than 10^{-3} for $m_C = 1.57 - 0.47i$ [*Haynes and Wagner,* 1981] and $m_C = 2 - i$ [*Janzen,* 1979]. In contrast to this, *Chýlek et al.* [1984] found a considerable influence of the soot volume fraction for optical properties of very optically thick clouds.

Second, we have tested a case with a soot activation of 0.01 as suggested by *Pitchford et al.* [1991]. The corresponding droplet characteristics are $d = 2.60$ μm, $N_{drop} = 7 \times 10^9$ m^{-3}, and $v = 10^{-5}$. For this contrail we found a grey color similar to that of the observed low-sulfur contrail, slightly less saturated. Thus, an activation of $a = 0.01$ cannot be excluded for contrail L from the computed color. However, the calculated optical depths $\tau(\lambda)$ are about 0.2 at most, a factor of about 3 times lower than computed for the contrail L with $a = 0.1$. Judged from the observations, $\tau \lesssim 0.2$ seems to be too low an optical depth, hence $a = 0.01$ may be regarded a lower boundary for the fraction of activated soot in the experiment, $a = 0.1$ beeing a more realistic value.

Third, we have repeated the calculations for a contrail that consists of frozen drops. Frozen drops are slightly larger than liquid ones because (1) the supersaturation relative to ice is larger than that relative to the liquid phase, and (2) ice has a lower density than water. The droplet sizes for an amount of 0.26 g kg^{-1} of depositionable vapor and an ice density of 0.9 g cm^{-3} are $d_{H,ice} = 0.71$ μm and $d_{L,ice} = 1.53$ μm for the high and low-sulfur contrails, respectively [see *Schumann et al.*, 1996, equation 2]. Since the frozen drops are larger, the soot volume fractions are lower than in liquid drops, namely, $v_{H,ice} = 4.9 \times 10^{-4}$ and $v_{L,ice} = 4.9 \times 10^{-5}$. The optical properties of these contrails were computed using refractive indices for ice from *Warren* [1984]. We found for the ice contrails similar wavelength dependencies than for the liquid water contrails, leading to similar colors (relativ differences in chromaticity coordinates less than 1.4%). The ice contrails are optically thicker than the corresponding water contrails, at some wavelengths by a factor of about 2. This shows that if the droplets would freeze very soon after the contrails become visible, we could not see it by a change of hue, but rather by a change of contrast (i.e., degree of darkness) against the background. However, the droplets need time to grow which smoothes contrast variations and makes them difficult to interprete.

6. Conclusions

In the present paper we have performed a more detailed analysis of the color effect that was observed during the second ATTAS experiment [*Schumann et al.*, 1996]. We have quantitatively determined the chromaticity coordinates of the colors of the low- and high-sulfur contrails. Then we have computed optical properties of the single droplets and of the whole contrails. For this, we used the scenario tentatively proposed by *Schumann et al.* [1996] for the explanation of the colors. We found that, indeed, the computed colors for the proposed scenario agree very well with the observed ones. This finding should corroborate the assumptions made by *Schumann et al.* [1996] about the droplet nucleation. However, one must keep in mind that it is not the soot content in the droplets that determines the color. Instead, the color is mainly controlled by the size distribution and number density of the droplets. We assume, so far, that these parameters are in turn controlled by the activation degree of the soot particles. Nonetheless, it might be possible that the sulfur alone could determine the droplet number density and size spectrum. This is not clear at present and, unfortunately, a check is not possible since it is not known how many and how large drops could form in the earliest jet phase from binary homogeneous H_2O/H_2SO_4 nucleation.

Furthermore, we have computed the colors of a contrail with a soot activation of $a = 0.01$ as suggested by *Pitchford et al.* [1991]. We found chromaticity coordinates similar to those of the L contrail, but about 3 times lower optical depths which, judged from the observations, seems to be too low. Thus from the color effect, a low soot activation degree as 0.01 cannot be excluded, yet this value should be regarded as a lower limit.

Finally, we have tested whether freezing of the droplets would be signalled by a color change. We found that freezing would let the hue remain almost unchanged, whereas it would result in larger optical thickness of the contrails, that is, darker appearance in front of the bright background. However, the optical depth of a contrail anyway increases in time because the droplets grow. Thus, the interpretation of an increasing contrast in terms of droplet freezing is difficult.

References

Appleman, H., The formation of exhaust condensation trails by jet aircraft, *Bull. Am. Meteorol. Soc., 34*, 14-20, 1953.

Busen, R., and U. Schumann, Visible contrail formation from fuels with different sulfur contents, *Geophys. Res. Lett., 22*, 1357-1360, 1995.

Chýlek, P., and J. Hallett, Enhanced absorption of solar radiation by cloud droplets containing soot particles in their surface, *Q. J. R. Meteorol. Soc., 118*, 167-172, 1992.

Chýlek, P., V. Ramaswamy, and R. J. Cheng, Effect of graphitic carbon on the albedo of clouds, *J. Atmos. Sci., 41*, 3076-3084, 1984.

DeMott, P. J., An exploratory study of ice nucleation by soot aerosols, *J. Appl. Meteorol., 29*, 1072-1079, 1990.

DIN 6164, Teil 1 u. 2: DIN-Farbenkarte. Beibl. 1-25: Farbmuster für Farbton 1 bis 24 und unbunte Farben, Beuth Verlag, Köln, 1960-62.

Hagen, D. E., M. B. Trueblood, and P. D. Whitefield, A field sampling of jet exhaust aerosols, *Partic. Sci. Technol., 10*, 53-63, 1992.

Hale, G. M., and M. R. Querry, Optical constants of water in the 200-nm to 200-μm wavelength region, *Appl. Opt., 12*, 555-563, 1973.

Haynes, B. S., and H. G. Wagner, Soot formation, *Progr. Energy Combust. Sci., 7*, 229-273, 1981.

Hofmann, D. J., and J. M. Rosen, Balloon observations of a particle layer injected by a stratospheric aircraft at 23 km, *Geophys. Res. Lett., 5*, 511-514, 1978.

Husar, R. B., and W. H. White, on the color of the Los Angeles smog, *Atmos. Environ., 10*, 199-204, 1976.

Janzen, J., The refractive index of colloidal carbon, *J. Colloid Interface Sci., 69*, 436-447, 1979.

Joseph, J. H., W. J. Wiscombe, and J. A. Weinmann, The delta-Eddington approximation for radiative flux transfer, *J. Atmos. Sci., 33*, 2452-2459, 1976.

Judd, D. B., and G. Wyszecki, *Color in Business, Science and Industry*, 3rd ed., 533 pp., John Wiley, New York, 1975.

Kärcher, B., Th. Peter, and R. Ottmann, Contrail formation: Homogeneous nucleation of H_2SO_4/H_2O droplets, *Geophys. Res. Lett., 22*, 1501-1504, 1995.

Kärcher, B., Th. Peter, U. M. Biermann, and U. Schumann, The initial composition of jet condensation trails, to appear, *J. Atmos. Sci.*, 1996.

Miake-Lye, R. C., R. C. Brown, M. R. Anderson, and C. E. Kolb, Calculations of condensation and chemistry in an aircraft contrail, in *DLR-Mitt. 94-06*, p. 274-279, DLR, D-51140 Köln, Germany, 1994.

Middleton, W. E. K., *Vision Through the Atmosphere*, 250 pp., Univ. of Toronto Press, Toronto, Ontario, 1952.

Parungo, F., B. Kopcewicz, C. Nagamoto, R. Schnell, P. Sheridan, C. Zhu, and J. Harris, Aerosol particles in the Kuwait oil fire plumes: Their morphology, size distribution, chemical composition, transport, and potential effect on climate, *J. Geophys. Res., 97*, 15,867-15,882, 1992.

Pitchford, M., J. G. Hudson, and J. Hallett, Size and critical supersaturation for condensation of jet engine exhaust particles, *J. Geophys. Res., 96*, 20,787-20,793, 1991.

Reiner, T., and F. Arnold, Laboratory flow reactor measurements of the reaction $SO_3+H_2O+M \rightarrow H_2SO_4+M$: Implications for gaseous H_2SO_4 and aerosol formation in the plumes of jet aircraft, *Geophys. Res. Lett., 20*, 2659-2662, 1993.

Richter, M., *Einführung in die Farbmetrik*, 274 pp., de Gruyter, Berlin, Germany, 1976.

Sassen, K., Iridescence in an aircraft contrail, *J. Opt. Soc. Am., 69*, 1080-1083 and 1194, 1979.

Schumann, U., On the effect of emissions from aircraft engines on the state of the atmosphere, *Ann. Geophys., 12*, 365-384, 1994.

Schumann, U., J. Ström, R. Busen, R. Baumann, K. Gierens, M. Krautstrunk, F. P. Schröder, and J. Stingl, In situ observations of particles in jet aircraft exhausts and contrails for different sulfur containing fuels, *J. Geophys. Res., 101*, 6853-6869, 1996.

Warren, S. G., Optical constants of ice from the ultraviolet to the microwave, *Appl. Opt., 23*, 1206-1225, 1984.

World Meteorological Organization (WMO), Scientific Assessment of Ozone Depletion: 1994, *Global Ozone Research and Monitoring Project - Rep. 37*, World Meteorol. Org., Geneva, Switzerland, 1995.

Wyslouzil, B. E., K. L. Carleton, D. M. Sonnenfroh, W. T. Rawlins, and S. Arnold, Observations of hydration of single, modified carbon aerosols, *Geophys. Res. Lett., 21*, 2107-2110, 1994.

Zhao, J., and R. P. Turco, Nucleation simulation in the wake of jet aircraft in stratospheric flight, *J. Aerosol Sci., 26*, 779-795, 1995.

K. Gierens and U. Schumann, Deutsche Forschungsanstalt für Luft- und Raumfahrt (DLR), Institut für Physik der Atmosphäre, Oberpfaffenhofen, D-82234 Wessling, Germany.

(Received August 29, 1995; revised February 29, 1996; accepted April 9, 1996.)